Impact of Polarization Diversity in Massive MIMO for Industry 4.0

Frédéric Challita, Pierre Laly, Martine Liénard
and Davy P. Gaillot
University of Lille/IEMN/Telice, Villeneuve D'Ascq, France
Email: frederic.challita@univ-lille.fr

Emmeric Tanghe and Joseph Wout
IMEC-WAVES, Ghent University
Ghent, Belgium
Email: wout.joseph@ugent.be

Abstract—The massive polarimetric radio channel is evaluated in an indoor industrial scenario at 3.5 GHz using a $10{\times}10$ uniform rectangular array (URA). The analysis is based on (1) propagation characteristics like the average received power and the power to interference ratio from the Gram matrix and (2) system-oriented metrics such as sum-rate capacity with maximum-ratio transmitter (MRT). The results clearly show the impact of polarization diversity in an industrial scenario and how it can considerably improve different aspects of the system design. Results for sum-rate capacity are promising and show that the extra degree of freedom, provided by polarization diversity, can optimize the performance of a very simple precoder, the MRT.

I. INTRODUCTION

New technologies for wireless communications are needed to tackle the ever-increasing requirements for the fifth-generation (5G) wireless systems [1]. Machine-to-Machine (M2M) communication systems, consist in a large number of separately organized devices connected through a network and can be used in different applications such as industrial automation, health care, logistics and electricity grids [2]. The ITU-R IMT-2020 (5G) vision [3] includes massive machine type communications (mMTC) as a usage scenario. The European Telecommunications Standards Institute (ETSI), IEEE and the Third Generation Partnership Project (3GPP) have also confirmed the need to support increasing number of M2M communications in Long Term Evolution (LTE) [4].

Massive MIMO (multiple-input multiple-output) is an emerging paradigm that uses the extra dimension of space to separate different receivers in the same time-frequency resource. When the number of transmitting antennas approaches infinity, user channels become orthogonal and simple linear precoding schemes can be applied [5]. Despite the fact that most measurements and field trials assume use-cases for enhanced mobile broadband (eMBB), this technology can be applied to other 5G use-cases such as internet of things (IOT) and M2M [6]. The advantages brought by massive MIMO make it a potential viable solution for industrial automation usage scenarios in the drive for the fourth industrial revolution or Industry 4.0 [7]. An overview of massive MIMO, opportunities and challenges can be found in [8], [9].

Sub-6 GHz bands are crucial to support most 5G scenarios. The 3.3-4.2 and 4.4-5 GHz ranges deliver the best compromise between wide coverage and spectral efficiency making them attractive for mMTC use-cases [10] in large indoor industrial

scenario for instance. Radio channel measurements are essential to derive the required design parameters of the wireless system. Hence, a better understanding of the propagation channel and underlying mechanisms (e.g. polarization diversity effects) in industrial environments is, therefore, not only of interest but certainly required.

Some works have investigated the radio channel in industrial environments. In [11], the authors present SISO (single input single output) measurements at 5.85 GHz for communication of industrial robots in an automation cell. In [12], an analysis of the polarization characteristics of specular and dense multi-path components in a large industrial hall at 1.3 GHz with 22-MHz bandwidth using RiMAX estimator are presented. Ultra-wideband measurements were also performed from 3.1 to 10.6 GHz in [13] and statistical models were established. These works mostly analyze the tap-delay profile parameters such as delay-spread, excess delay, path-loss and received power. Pathloss, shadowing measurements and capacity analysis for industrial indoor environments for three different industrial indoor environments at 900, 1600, and 2450 MHz are presented in [14]. A comparison between the system performance at 1.3, 3.5 and 6 GHz was presented in [15] for the same industrial scenario investigated in this work.

Based on this literature review, it can be safely concluded that polarimetric massive MIMO channel measurements in industrial environments are clearly missing. The compromise between the use of polarization diversity to separate users and the drop in average received power should be clearly identified via propagation and system metrics. From this discussion, the goal of this study is to experimentally evaluate the massive MIMO channel at 3.5 GHz for different use-cases in the industrial environment. The discussion is twofold: (1) the dependence of the channel characteristics on the considered scenario especially when polarization diversity is considered and (2) the overall performance of the system with the combined effect of spatial multiplexing and polarization diversity. This is done using propagation based metrics (average received power and power to interference ratio) and system-oriented metrics such as sum-rate capacity with MRT to evaluate the overall performance of massive MIMO in given use-cases inside an industrial scenario for potential mMTC.

The rest of the paper is organized as follows: the industrial environment, measurement setup and the channel sounding

procedure are outlined in section II. Section III presents the different evaluation metrics and the results are presented in section IV before concluding in Section V.

1) Notations: In this paper, $(.)^H$ represents the Hermitian matrix (conjugate transpose), $|.|$ is the absolute value (magnitude), $\|.\|$ the norm of a vector and $\|.\|_F$ the Frobenius norm of a matrix. Lower case letters are used to denote scalars and boldface is used to denote vectors. Upper case boldface letters represent matrices. I.i.d. denotes the independent and identically elements distribution. K is the number of receivers and M the number of elements in the transmitting array.

II. MEASUREMENT SETUP

A. Measurement Environment

The propagation environment is a large industrial hall located in Technologiepark-Zwijnaarde, Belgium. The $21.3 \times 77.2 \times 12.2 \ m^3$ hall is a research lab dedicated for testing the robustness of concrete structures. The dominant building material for walls, floor, and ceiling is concrete. The windows are located near the ceiling and a large metallic industrial door which was closed during the measurements is located at the end of the hall. Large metallic machines and measurement tools can be found in the environment which is typical for an automation cell for instance inside an industrial building. In Fig. 1(a), a panoramic view from the Tx array is shown.

B. Scenario

The massive MIMO scenario is a multi-user massive MISO (MU-MISO) setup where a number of single antenna receivers are distributed in the industrial hall as illustrated in Fig. 1(b). The transmitter is a massive virtual vertical uniform rectangular array (URA) created by moving an antenna along a metallic rail. The positioning system is commanded via fiber optics and a dedicated LabView program installed on a Windows PC. The separation between array elements was set to 0.45λ at 3.5 GHz. The different sounding parameters and characteristics of the Tx array are listed in Table I.

TABLE I
SOUNDING PARAMETERS AND TX ARRAY CHARACTERISTICS.

VNA	Frequency	3.5 GHz
	Span Bandwidth	80 MHz
	Maximum resolvable path	3.75 m
	Number of frequency points M_f	819
	Number of observations N_{obs}	20
	Tx Power	3 dBm
Tx array	URA dimension	10×10
	Tx spacing	3.86 cm
	Tx Height	6.5 m
	Rx Height	1.6 m

The distribution of the different receiver locations and the three scenarios are described hereafter:

1) Rx 1 to 6 : uniformly arranged machines or industrial robots in straight line along y-direction with line-of-sight (LOS).

(a)
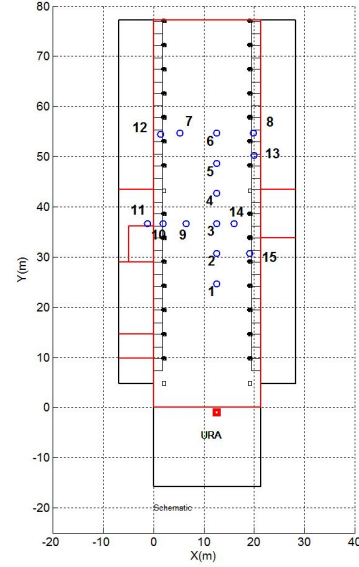
(b)

Fig. 1. a) Panoramic view of the industrial hall from the Tx point of view and b) Schematic of the distributed setup

2) Rx 3, 9, 10, 11, 14 : distributed machines or industrial robots: LOS, obstructed LOS (OLOS), non-LOS (NLOS) along x-direction and contains a severe NLOS case (Rx 11).

3) Positions in this third scenario (7, 8, 10, 11, 13 and 15) are randomly chosen to provide a distribution of user channels with severe NLOS (SNLOS) and high concentration of concrete and metal around the antenna (Rx 8), obstructed LOS (e.g. Rx 7 and 10).

The three separate scenarios can be considered as three different use-cases for automation cells. This selection allows a thorough evaluation of the propagation channel in a large industrial scenario with a massive MIMO setup.

C. Radio Channel Sounding

Radio Channel sounding measurements were performed in the frequency domain using a vector network analyzer (VNA) of reference Agilent E5071C (see parameters in Table I). A 500-m optical fiber was deployed for the receiving side with an RF (radio frequency) to optical/optical to RF interface to allow

the Rx to move within a 500-m radius of the Tx. A power amplifier is used at Tx side and a LNA (low noise amplifier) at receiver end. The system was through (S_{21}) calibrated (without the antennas and power amplifier) to mitigate the impact of the system (Tx and Rx frontend and connection cables). Power amplifier effects were eliminated in post-processing.

1) Antennas: Identical mono-polarized patch antennas were used and manually rotated to get both polarizations. The cross-polarization factor of these antennas is around 15 dB. These antennas operate at 3.5 GHz center frequency with 80 MHz bandwidth, 80 degrees beamwidth at -3 dB (in azimuth and elevation), 7 dBi gain and typical nominal VSWR ≤ 2 in the band of interest. Polarization diversity was applied only at the Tx level.

2) Polarimetric Massive MIMO Channel Matrix: For each Rx position k, Tx antenna m and polarization link ψ, the wideband complex channel transfer function $\mathbf{h}_{k,m,\psi}(f) \in \mathbb{C}^{1 \times M_f}$ is obtained from the S_{21} parameter, where $k = 1, 2, ..., K$, $m = 1, 2, ..., M$, and M_f is the total number of frequency points, respectively. ψ can be either co-polar VV or cross-polar HV, the first letter denoting Tx polarization and the second Rx polarization. The polarimetric MU-MISO channel matrix $\mathbf{H}_\psi \in \mathbb{C}^{K \times M \times M_f}$ is constructed from $\mathbf{h}_{k,m,\psi}$ for all possible k and m values.

III. EVALUATION METRICS

a) Average Received Power: The polarimetric average received power for each Tx-Rx link $\mathcal{P}_{m,k}(\psi)$ is first computed in the bandwidth B_w and is given by :

$$\mathcal{P}_{k,m}(\psi) = \frac{1}{M_f} \sum_{i=1}^{M_f} \left(|\mathbf{h}_{k,m,\psi}(i)|^2 \right). \qquad (1)$$

b) Power to Interference Ratio: A classical metric to evaluate the performance of massive MIMO is the power to interference ratio (PTI) computed from the $K \times K$ Gram matrix $\mathbf{G} = \mathbf{H}\mathbf{H}^H$ for each frequency bin. This metric indicates what is the percentage of the transmitted power that actually reaches a given receiver instead of interfering with different users. It shows how favorable the propagation environment is for the deployment of a massive MIMO system. The PTI ratio $\gamma_k(\mathbf{G})$ for user k can be formulated as :

$$\gamma_k(\mathbf{G}) = \frac{|g_{k,k}|^2}{\sum_{j=1}^{K} |g_{k,j}|^2} \qquad (2)$$

c) Sum-rate Capacity: The sum-rate in the considered scenario provides an insight into the spectrum efficiency sharing among the different users. The achievable ergodic rate is a logarithmic function of the $SINR$ (signal-to-noise-plus-interference ratio). Here the signal is precoded and the power is equally distributed amongst users. For user k :

$$C_k = \log_2(1 + SINR_k), \quad in \ bits/s/Hz \qquad (3)$$

and the $SINR_k$ can be found as :

$$SINR_k = \frac{p_k |\mathbf{h}_k \mathbf{w}_k|^2}{\sum_{i=1, \ i \neq k}^{K} p_i |\mathbf{h}_k \mathbf{w}_i|^2 + \sigma_n^2}, \qquad (4)$$

where p_k designates power allocated to the kth user and $\mathbf{w}_k$ the precoding vector. The sum-rate capacity is obtained by summing the rates of the different users. From Eqs. 2 and 3, it can be seen that the systems performance increases when the signal is enhanced and interference is suppressed. This is an overall system performance metric as opposed to power to interference ratio for which the scenario dependency and channel influence can be seen at the level of each receiver.

d) Channel Normalization: For sum-rate capacity, channel normalization is applied carefully to keep the imbalance between both polarizations for capacity analysis. Consider $\mathbf{H}$ the $K \times M$ channel matrix, then the normalization is as follows:

$$\mathbf{H}_{VV}^n = \frac{\sqrt[2]{KM} \ \mathbf{H}_{VV}}{||\mathbf{H}_{VV}||_F} \quad and \quad \mathbf{H}_{HV}^n = \frac{\sqrt[2]{KM} \ \mathbf{H}_{HV}}{||\mathbf{H}_{VV}||_F}. \qquad (5)$$

IV. RESULTS

Fig. 2 shows the co- and cross- $|\mathbf{h}(f)|^2$ for positions 1 (strong LOS) and 8 (severe NLOS, high metal concentration around the receiver) for one Tx-Rx link to highlight the particularity of this type of environments. Indeed, different receivers exhibit rather different fading characteristics. It also demonstrates the degree of diversity brought by polarization diversity compared to a nearly flat co-polar channel in LOS conditions (Rx1). Fig. 3 presents a boxplot of the received gain
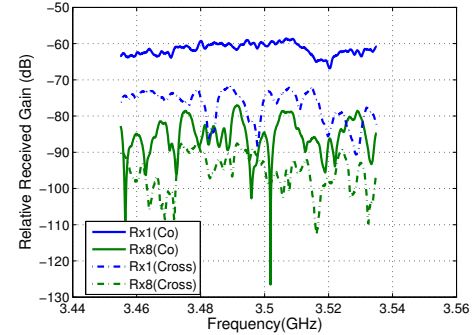

Fig. 2. $|\mathbf{h}(f)|^2$ for two positions in the scenario for co- and cross-polarization links

for each Rx position where the central mark is the median, the edges are the 25th and 75th percentiles and outliers points are plotted individually using red crosses, respectively. Note that the plot is a function of distance and not following the numbering of the receivers as in Fig. II-B. It can be seen (1) that power variations across Tx array can reach high values (up to 10 dB in some cases). It is concluded that large scale fading occurs at the transmitter side which is not the case for simple MIMO case. Similar observations were reported in [16]. Moreover, (2) shadowing effects can be observed for Rx 3 (located at point A around 38 m) where a section of the Tx array is obstructed from the receiver explaining the large spread of power across Tx. This spatial non-stationarity effect should be accounted for in industrial channel models as it can greatly impact the performance of the system.
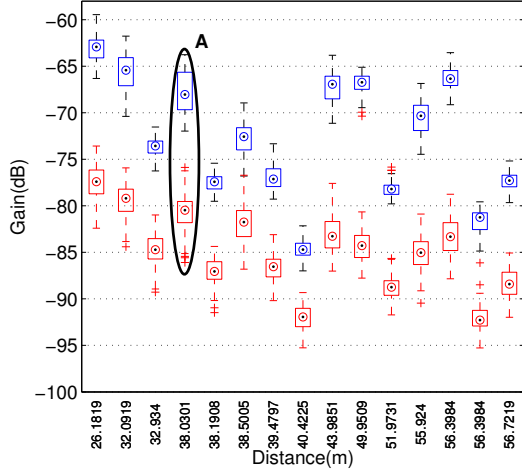
Fig. 3. Average received power in co and cross-polarization across the array

In Fig. 4, the PTI is presented for the different users in each of the selected scenarios described in II-B. Fig. 4(a) presents the PTI dependence to the distance whereas (b) and (c) show the dependence to the corresponding user positions (Sec. II(b)). The different labels indicate the identified shadowing scenario (LOS, NLOS, OLOS and SNLOS) for each Rx. It can be observed from Fig. 4(a) that cross-polarization
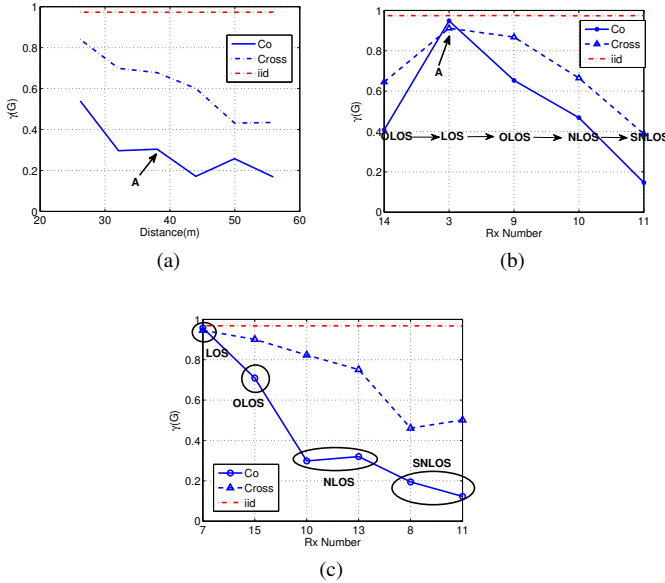

Fig. 4. PTI ratio of the different receivers for (a) Scenario 1, (b) Scenario 2 and (c) Scenario 3

schemes drastically improve the PTI ratio. It is also shown that this ratio decreases with distance which was expected because the average received power is subsequently lower. However, it still has improvement over co-polarized schemes in strong LOS scenario wherein users channels are spatially correlated and spatial separation is more challenging than in NLOS conditions. This proves that interference reduction

is a very important aspect to optimize the performance of the different users channels and that the extra degree of freedom provided by polarization diversity alongside spatial multiplexing is crucial to massive MIMO setups in the studied scenario. It should be noted that if the received useful power is low and interference power is also low, the PTI would still be high. However, the range of average received power values observed earlier is still sufficient for cross-polarization links meaning interference reduction mostly contributes to decorrelate the different channels. From Fig. 4(b), it can be seen that interference reduction and power focusing depends heavily on the Rx position and considered scenario, thus on the propagation channel and its characteristics. For instance, Rx3 clearly present different behaviors whether it belongs to scenario 1 or 2 (point A in Fig. 3 and Fig. 4(a) and (b)). A PTI value close to 0.9 is observed in Scenario 2 whereas this ratio is around 0.67 (cross) and 0.30 (co) for Scenario 1 for which the users have higher correlations. This underlines the importance of polarization diversity especially when spatial correlation between the users is high and the use of co-polarization leads to more interference and thus lower PTI ratio. The same conclusion stands for Rx11 where a great improvement is observed with cross-polarization ($\approx 50\%$).

In Fig. 5, the sum-rate capacity is presented as a function of the number of Tx antennas for a signal-to-noise ratio (SNR) of 20 dB. For the sake of comparison, the same number of users was considered for scenarios 1 and 3. From this figure, it can be observed that increasing the number of transmitting elements generally increases the sum-rate capacity of the system as expected in massive MIMO systems. Also, the diversity brought by polarization is demonstrated with the sum-rate capacity for cross-polarized schemes being always larger than for co-polar despite less average received power. It follows less antennas are needed to achieve a given spectral efficiency with cross-polarization. For instance, in scenario 1, all 100 Tx antennas are needed to reach ≈ 5 bps/Hz whereas less than 25 are needed if cross-polarization is used. This is well-pronounced for scenario 1 where the sum-rate does not increase with the number of Tx elements in co-polar. This is a straightforward example of use-cases where the need for an extra degree of freedom is needed in this complex propagation environment. Another important observation, is the influence of the propagation environment on the capacity curves. For instance, comparing scenario 1 and 3, nearly the same capacity is achieved with cross-polar even though users in scenario 1 have higher correlation and users in scenario 3 are more distributed. Finally, it is noteworthy reducing the interference in such use-cases is critical. As a matter of fact for the studied environment, having more received power and adding more antennas do not necessarily increase the sum-rate capacity.

V. CONCLUSION

In this work, polarimetric channel measurements of a MU-MISO setup for an indoor industrial scenario are presented at 3.5 GHz with 80 MHz bandwidth. The scenario consists in a massive URA transmitter and three use-cases with different
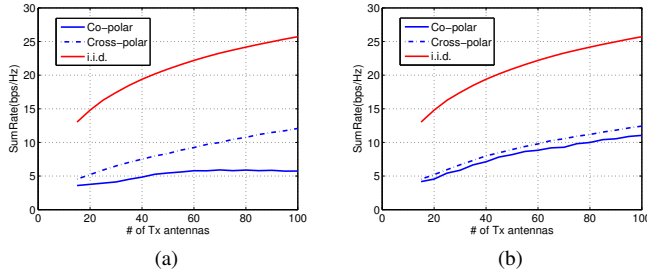
Fig. 5. Sum-rate capacity for (a) Scenario 1 and (b) Scenario 3

number and distribution of users. The industrial massive channel was evaluated using propagation metrics (average received power and PTI) and system oriented metrics (sum-rate capacity). It was shown from the PTI analysis the polarization diversity impact for massive MIMO setups. This extra degree of freedom brings richness and diversity at the channel level and is observed to contribute to the decorrelation between users. Good sum-rate capacity results were obtained using MRT with cross-polarization even when less antennas are active (i.e. less RF chains if digital beamforming is considered). Therefore, the simplicity provided by MRT and improvement brought by polarization diversity to improve the spectral efficiency can greatly benefit to massive MIMO setups for indoor industrial environments. Future works include the evaluation of antenna selection strategies for different use-cases and frequency bands to further optimize the overall performance using less RF chains.

REFERENCES

[1] M. Agiwal, A. Roy, and N. Saxena, "Next generation 5g wireless networks: A comprehensive survey," *IEEE Communications Surveys Tutorials*, vol. 18, no. 3, pp. 1617–1655, thirdquarter 2016.

[2] Y. Zhang, R. Yu, M. Nekovee, Y. Liu, S. Xie, and S. Gjessing, "Cognitive machine-to-machine communications: visions and potentials for the smart grid," *IEEE Network*, vol. 26, no. 3, pp. 6–13, May 2012.

[3] ITU, *Recommendation ITU-R M.2083, "IMT Vision Framework and overall objectives of the future development of IMT for 2020 and beyond"*. [Online]. Available: https://www.itu.int/dms_pubrec/itu-r/rec/m/R-REC-M.2083-0-201509-I!!PDF-E.pdf

[4] CISCO, *Cisco Visual Networking Index: Global Mobile Data Traffic Forecast Update, 2016-2021*. [Online]. Available: https://www.cisco.com/c/en/us/solutions/collateral/service-provider/visual-networking-index-vni/mobile-white-paper-c11-520862.pdf

[5] T. L. Marzetta, "Noncooperative cellular wireless with unlimited numbers of base station antennas," *IEEE Transactions on Wireless Communications*, vol. 9, no. 11, pp. 3590–3600, November 2010.

[6] G. A. Akpakwu, B. J. Silva, G. P. Hancke, and A. M. Abu-Mahfouz, "A survey on 5g networks for the internet of things: Communication technologies and challenges," *IEEE Access*, vol. 6, pp. 3619–3647, 2018.

[7] S. K. Rao and R. Prasad, "Impact of 5g technologies on industry 4.0," *Wirel. Pers. Commun.*, vol. 100, no. 1, pp. 145–159, May 2018. [Online]. Available: https://doi.org/10.1007/s11277-018-5615-7

[8] L. Lu, G. Y. Li, A. L. Swindlehurst, A. Ashikhmin, and R. Zhang, "An overview of massive mimo: Benefits and challenges," *IEEE Journal of Selected Topics in Signal Processing*, vol. 8, no. 5, pp. 742–758, Oct 2014.

[9] F. Rusek, D. Persson, B. K. Lau, E. G. Larsson, T. L. Marzetta, O. Edfors, and F. Tufvesson, "Scaling up mimo: Opportunities and challenges with very large arrays," *IEEE Signal Processing Magazine*, vol. 30, no. 1, pp. 40–60, Jan 2013.

[10] Huawei, "5g spectrum," 2018, https://www-file.huawei.com/-/media/CORPORATE/PDF/public-policy/public_policy_position_5g_spectrum.pdf.

[11] B. Holfeld, D. Wieruch, L. Raschkowski, T. Wirth, C. Pallasch, W. Herfs, and C. Brecher, "Radio channel characterization at 5.85 ghz for wireless m2m communication of industrial robots," in *2016 IEEE Wireless Communications and Networking Conference*, April 2016, pp. 1–7.

[12] D. P. Gaillot, E. Tanghe, W. Joseph, P. Laly, V. Tran, M. Liénard, and L. Martens, "Polarization properties of specular and dense multipath components in a large industrial hall," *IEEE Transactions on Antennas and Propagation*, vol. 63, no. 7, pp. 3219–3228, July 2015.

[13] J. Karedal, S. Wyne, P. Almers, F. Tufvesson, and A. F. Molisch, "A measurement-based statistical model for industrial ultra-wideband channels," *IEEE Transactions on Wireless Communications*, vol. 6, no. 8, pp. 3028–3037, August 2007.

[14] Y. Ai, M. Cheffena, and Q. Li, "Radio frequency measurements and capacity analysis for industrial indoor environments," in *2015 9th European Conference on Antennas and Propagation (EuCAP)*, April 2015, pp. 1–5.

[15] F. Challita, P. Laly, M. Liénard, D. Gaillot, E. Tanghe, and W. Joseph, "Massive mimo for industrial scenarios: Measurement-based polarimetric analysis," *European Cooperation in Science and Technology EURO-COST Dublin, Ireland*, 2019.

[16] S. Payami and F. Tufvesson, "Channel measurements and analysis for very large array systems at 2.6 ghz," in *2012 6th European Conference on Antennas and Propagation (EUCAP)*, March 2012, pp. 433–437.